

Novel method for identifying the heaviest QED atom

Jing-Hang Fu,^{1,*} Sen Jia,^{2,*} Xing-Yu Zhou,³ Yu-Jie Zhang,^{1,4,†} Cheng-Ping Shen,^{5,6,‡} and Chang-Zheng Yuan^{7,8,§}

¹*School of Physics, Beihang University, Beijing 100083, China*

²*School of Physics, Southeast University, Nanjing 211189, China*

³*School of Physics and Electronic Technology, Liaoning Normal University, Dalian 116029, China*

⁴*Peng Huanwu Collaborative Center for Research and Education, Beihang University, Beijing 100191, China*

⁵*Key Laboratory of Nuclear Physics and Ion-beam Application (MOE) and Institute of Modern Physics, Fudan University, Shanghai 200443, China*

⁶*School of Physics, Henan Normal University, Xinxiang 453007, China*

⁷*Institute of High Energy Physics, Chinese Academy of Sciences, Beijing 100049, China*

⁸*University of Chinese Academy of Sciences, Beijing 100049, China*

QED atoms are composed of unstructured and point-like lepton pairs bound together by the electromagnetic force. The smallest and heaviest QED atom is formed by a $\tau^+\tau^-$ pair. Currently, the only known atoms of this type are the e^+e^- and μ^+e^- atoms, which were discovered 64 years ago and remain the sole examples found thus far. We demonstrate that the J_τ ($\tau^+\tau^-$ atom with $J^{PC} = 1^{--}$) atom signal can be observed with a significance larger than 5σ including both statistical and systematic uncertainties, via the process $e^+e^- \rightarrow X^+Y^-\cancel{E}$ ($X, Y = e, \mu, \pi, K, \text{ or } \rho$, and \cancel{E} is the missing energy due to unobserved neutrinos) with 1.5 ab^{-1} data taken around the τ pair production threshold. The τ lepton mass can be measured with a precision of 1 keV with the same data sample. This is within one year's running time of the proposed super tau-charm facility in China or super charm-tau factory in Russia.

Keywords: QED atom, Tau lepton, e^+e^- annihilation, STCF, SCTF

1. Introduction

Quantum electrodynamics (QED) atoms are formed of lepton pairs (e^+e^- , μ^+e^- , τ^+e^- , $\mu^+\mu^-$, $\tau^+\mu^-$, and $\tau^+\tau^-$) by electromagnetic interactions, similar to hydrogen formed of a proton and an electron. Their properties have been studied to test QED theory [1, 2], fundamental symmetries [3, 4], gravity [5, 6], and search for physics beyond the Standard Model [4, 7–9], and so on. The first QED atom was discovered in 1951, which is the e^+e^- bound state and named positronium [10]; the second one was discovered in 1960, which is the μ^+e^- bound state and named muonium [11]. No other QED atom was found in the past 64 years. New colliders are proposed to discover the true muonium [12, 13] which decays into final states with electrons and photons [14, 15]. The heaviest and smallest QED atom, a bound state of $\tau^+\tau^-$ [16], is named tauonium [17, 18], ditauonium [19, 20], or true tauonium [21]. We classify the bound states of $\tau^+\tau^-$ following the charmonium spectroscopy [22] simply as $J_\tau(nS)$, $\eta_\tau(nS)$, and $\chi_{\tau J}(nP)$ for the states with quantum numbers of n^3S_1 , n^1S_0 , and $(n+1)^3P_J$, respectively. Here, n is the radial quantum number, and S and P denote the orbital angular momentum of 0 and 1, respectively. There were many theoretical studies in the literature since the discovery of the τ lepton. The spec-

troscopy of $\tau^+\tau^-$ atoms was studied in Ref. [19]. The production of η_τ was considered in Refs. [20, 21] and that of the process $e^+e^- \rightarrow J_\tau(1S) \rightarrow \mu^+\mu^-$ in Refs. [17, 23, 24]. In addition, study of the $J_\tau(nS)$ via the processes $e^+e^- \rightarrow J_\tau(1S) \rightarrow$ light hadrons [17, 18] and $e^+e^- \rightarrow J_\tau(nS) \rightarrow \gamma\eta_\tau$ were proposed [16]. Achievements have been made in the precise measurements of standard model and searches for exotic states at e^+e^- colliders [25–31].

2. Methods and calculations

In this Letter, we introduce a novel method for identifying $J_\tau(nS)$ by measuring the cross section ratio $\sigma(e^+e^- \rightarrow X^+Y^-\cancel{E})/\sigma(e^+e^- \rightarrow \mu^+\mu^-)$. Here $X, Y = e, \mu, \pi, K, \text{ or } \rho$, and \cancel{E} is the missing energy due to unobserved neutrinos. To suppress backgrounds with extra missing particles, one can require no additional photons in the event besides those from ρ decays and the number of good charged tracks is exactly two for all the channels of $\tau\tau \rightarrow ee, e\mu, e\pi, eK, \mu\mu, \mu\pi, \mu K, \pi K, \pi\pi, KK, e\rho, \mu\rho, \text{ and } \pi\rho$. To remove background events from two-photon processes of $e^+e^- \rightarrow e^+e^-e^+e^-$ and $e^+e^- \rightarrow e^+e^-\mu^+\mu^-$, a lower limit of the transverse momentum of the charged tracks can be applied. The process of $e^+e^- \rightarrow X^+Y^-\cancel{E}$ can manifest in intermediate states in two distinct ways: $\tau^+\tau^-$ open states above the double τ lepton mass threshold ($2m_\tau$) and $\tau^+\tau^-$ bound states $J_\tau(nS)$ just below the threshold with a binding energy of $E_n \approx \alpha^2 m_\tau / (4n^2) \approx 23.7/n^2 \text{ keV}$.

By fitting the $\sigma(e^+e^- \rightarrow X^+Y^-\cancel{E})/\sigma(e^+e^- \rightarrow \mu^+\mu^-)$ distribution in the vicinity of the τ pair production threshold with

*These authors contributed equally to this work.

†zyj@buaa.edu.cn (Corresponding author)

‡shencp@fudan.edu.cn (Corresponding author)

§yuancz@ihep.ac.cn (Corresponding author)

and without a $J_\tau(nS)$ atom component, we can identify its existence. We show below that the τ lepton mass measured with the process $e^+e^- \rightarrow \tau^+\tau^- \rightarrow X^+Y^-\cancel{E}$ will also be affected after considering the $J_\tau(nS)$ contribution.

The τ lepton mass is one of the fundamental parameters of the Standard Model. A precise τ mass measurement is essential to check the lepton flavor universality and constrain the ν_τ mass [32]. In the previous measurements of $e^+e^- \rightarrow \tau^+\tau^-$ cross sections at the BESIII [25–27] and KEDR experiments [28], the contribution of $e^+e^- \rightarrow J_\tau(nS)$ was not included in theoretical calculation. This is not a problem at these experiments as the uncertainties are at 100 keV level (The current world average value of τ mass is $m_\tau^{\text{PDG}} = (1776.86 \pm 0.12)$ MeV [22] and the recent most precise measurement from Belle II experiment is $1777.09 \pm 0.08 \pm 0.11$ MeV [33]), but the effect should not be ignored in the next generation experiments which aim at a precision of one or two orders of magnitude better than previous ones. In BESIII measurement [25], the primary source of systematic uncertainty arises from the energy scale and efficiency. In KEDR measurement [27], the primary systematic uncertainty is attributed to efficiency and luminosity measurements. In the next generation of experiments, the statistical uncertainty is anticipated to decrease due to the large integrated luminosity, while the systematic uncertainty will be mitigated through the adoption of new fitting methods developed in this work and the application of advanced technologies to the detector and accelerator design.

The cross section $\sigma(e^+e^- \rightarrow X^+Y^-\cancel{E})$ around the $\tau^+\tau^-$ production threshold is [25–28]

$$\sigma(W, m_\tau, \Gamma_\tau, \delta_W) = \int_{m_{J_\tau}}^{\infty} dW' \frac{1}{\sqrt{2\pi}\delta_W} e^{-\frac{(W-W')^2}{2\delta_W^2}} \times \int_0^{1-\frac{m_\tau^2}{W'^2}} dx F(x, W') \frac{\bar{\sigma}(W' \sqrt{1-x}, m_\tau, \Gamma_\tau)}{|1 - \Pi(W' \sqrt{1-x})|^2}. \quad (1)$$

Here, W is the center-of-mass energy, δ_W is the center-of-mass energy spread, $F(x, W)$ is the initial state radiation factor [34], $\Pi(W)$ is the vacuum polarization factor [35], and $\bar{\sigma}(W, m_\tau, \Gamma_\tau)$ is the Born cross section. With $J_\tau(nS)$ atoms included, Eq. (1) differs from those given in Refs. [25–28], where $2m_\tau$ is replaced by the ground state mass m_{J_τ} in the range of integration, the τ width Γ_τ is added as a variable, and the contribution of $J_\tau(nS)$ atoms ($\bar{\sigma}^{J_\tau}(W)$) is included in $\bar{\sigma}(W, m_\tau, \Gamma_\tau)$ as

$$\bar{\sigma}(W, m_\tau, \Gamma_\tau) = \bar{\sigma}^{J_\tau}(W) + \bar{\sigma}^{\text{con.}}(W), \quad (2)$$

where $\bar{\sigma}^{\text{con.}}(W)$ is the cross section from the $e^+e^- \rightarrow \tau^+\tau^-$ continuum process and is calculated to the next-to-leading order (NLO) in the fine structure constant α , as has been done for $\bar{\sigma}^{J_\tau}(W)$.

At NLO [14, 19], the cross section $\bar{\sigma}^{J_\tau}$ from narrow atoms is given by the Breit-Wigner function [22]

$$\bar{\sigma}^{J_\tau}(W) = \sum_n \frac{6\pi^2 |1 - \Pi(2m_\tau)|^2 \left(1 - \frac{3\alpha}{4\pi}\right)}{W^2 \Gamma_{\text{total}}^{J_\tau(nS)}} \times \delta(W - m_{J_\tau(nS)}) \Gamma_{X^+Y^-\cancel{E}}^{J_\tau(nS)} \times \Gamma_{e^+e^-}^{J_\tau(nS)}, \quad (3)$$

where $m_{J_\tau(nS)} = 2m_\tau - E_n$ is the mass of $J_\tau(nS)$, $|1 - \Pi(2m_\tau)|^2 (1 - 3\alpha/4\pi)$ is recalled here since the initial state radiation factor and the vacuum polarization factor have been considered in Eq. (1), $\Gamma_{X^+Y^-\cancel{E}}^{J_\tau(nS)}$ is the partial decay width of $J_\tau(nS) \rightarrow X^+Y^-\cancel{E}$, and $\Gamma_{e^+e^-}^{J_\tau(nS)}$ is that of $J_\tau(nS) \rightarrow e^+e^-$. We have

$$\begin{aligned} \Gamma_{e^+e^-}^{J_\tau(nS)} &= \frac{\alpha^5 m_\tau}{6n^3 |1 - \Pi(2m_\tau)|^2} \left(1 - \frac{13\alpha}{4\pi} + C_{\text{coulomb}}^{nS} \frac{\alpha}{\pi}\right), \\ \Gamma_{X^+Y^-\cancel{E}}^{J_\tau(nS)} &= 2\Gamma_\tau + \Gamma(J_\tau(nS) \rightarrow \gamma\chi_{\tau J}), \text{ and} \\ \Gamma_{\text{total}}^{J_\tau(nS)} &= \Gamma_{X^+Y^-\cancel{E}}^{J_\tau(nS)} + (2 + R)\Gamma_{e^+e^-}^{J_\tau(nS)}. \end{aligned} \quad (4)$$

Futher detailed data are available in Table 1, which is calculated to NLO in the fine structure constant α [19, 36]. Here, $2\Gamma_\tau$ is twice the free- τ decay width (since the lifetime of the bound state is about 10 times shorter than that of its components and relativistic corrections are neglected due to their minute contributions of the order of 10^{-4}). The uncertainties of R and Γ_τ are included in the theoretical uncertainties. The factor $(2 + R)$ comes from e^+e^- , $\mu^+\mu^-$, and hadronic final states with $R_{\text{exp.}} = 2.342 \pm 0.064$ [37], the total τ decay width $\Gamma_\tau = 2.2674 \pm 0.0039$ meV [22], and $\Gamma(J_\tau(nS) \rightarrow \gamma\chi_{\tau J})$ is the $E1$ transition width (the annihilation decays of $\chi_{\tau J}$ are ignored since their contributions are smaller than $\bar{\sigma}^{J_\tau}(W)$ by a factor of 10^{-6}). With Green functions, the Coulomb corrections (C_{coulomb}^{nS}) are calculated to be 5.804, 4.428, 3.810, 3.518, 3.358, 3.256, 3.186, 3.134, 3.093, and 3.061 for $n = 1, 2, 3, 4, 5, 6, 7, 8, 9$, and 10, respectively.

Most of the NLO corrections of $\Gamma(J_\tau(nS) \rightarrow e^+e^-)$ come from the vacuum polarization factor Π . Then we get

$$\bar{\sigma}^{J_\tau}(W) = (3.11 \pm 0.02) \delta\left(\frac{W - 2m_\tau + 13.8 \text{ keV}}{1 \text{ MeV}}\right) \text{ pb}, \quad (5)$$

where $13.8 \text{ keV} = \sum_n E_n Br_{X^+Y^-\cancel{E}}^{J_\tau(nS)} \Gamma_{e^+e^-}^{J_\tau(nS)} / \sum_n Br_{X^+Y^-\cancel{E}}^{J_\tau(nS)} \Gamma_{e^+e^-}^{J_\tau(nS)}$ with $Br_{X^+Y^-\cancel{E}}^{J_\tau(nS)}$ being the branching fraction of $J_\tau(nS) \rightarrow X^+Y^-\cancel{E}$. The uncertainty from R is one order of magnitude greater than that from m_τ and Γ_τ .

TABLE 1: The decay data of $J_\tau(nS)$ in meV.

n	$\Gamma_{e^+e^-}^{J_\tau(nS)}$	$2\Gamma_\tau$	$\Gamma_{E1}^{J_\tau(nS)}$	$\Gamma_{\text{total}}^{J_\tau(nS)}$	$\Gamma_{e^+e^-}^{J_\tau(nS)} Br_{X^+Y^-\cancel{E}}^{J_\tau(nS)}$
1	6.484	4.535	0.0000	32.695	0.899
2	0.808	4.535	0.0000	8.044	0.455
3	0.239	4.535	0.0072	5.573	0.195
$\sum_{n=1}^{\infty}$					1.795 ± 0.012

We use the NLO cross sections $\bar{\sigma}^{\text{con.}}(W)$ and take next-to-next-to-leading order (NNLO) corrections as uncertainties here [38]. To reduce the uncertainties from the initial state radiation factor and the vacuum polarization factor in Eq. (1), and that from the integrated luminosity [37], we introduce $R_{X^+Y^-\cancel{E}}$, ratio of the cross sections, as

$$R_{X^+Y^-\cancel{E}}(W, \delta_W, m_\tau) = \frac{\sigma(W, m_\tau, \Gamma_\tau, \delta_W)}{\sigma^{\mu^+\mu^-}(W, \delta_W)}. \quad (6)$$

Here, $\sigma^{\mu^+\mu^-}(W, \delta_W)$ is calculated with $\bar{\sigma}^{\mu^+\mu^-}(W) = \frac{4\pi\alpha^2(1+3\alpha/4\pi)}{3W^2}$ in Eq. (1). The higher order correction terms, such as $9\alpha m_\mu^2/\pi W^2$ and m_μ^4/W^4 , are ignored because they are merely global factors of about 2×10^{-5} here. With $m_\tau = m_\tau^{\text{PDG}}$ and $\delta_W = 1$ MeV [39], the cross sections $\sigma^{\text{atom}}(m_\tau^{\text{PDG}})$, $\sigma^{\text{con.}}(m_\tau^{\text{PDG}})$, and $\sigma^{\text{total}}(m_\tau^{\text{PDG}})$ are shown in Fig. 1.

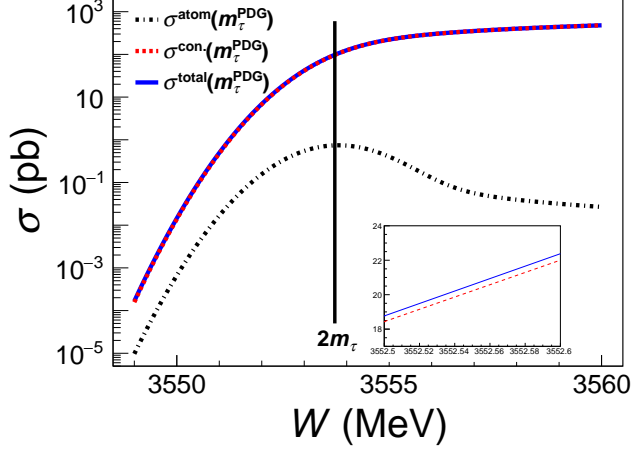


FIG. 1: Cross sections $\sigma^{\text{atom}}(m_\tau^{\text{PDG}})$, $\sigma^{\text{con.}}(m_\tau^{\text{PDG}})$, and $\sigma^{\text{total}}(m_\tau^{\text{PDG}})$ as a function of center-of-mass energy W . The black vertical line shows the $\tau^+\tau^-$ mass threshold. The inset shows the $\sigma^{\text{con.}}(m_\tau^{\text{PDG}})$ and $\sigma^{\text{total}}(m_\tau^{\text{PDG}})$ as a function of W in a small W region of 3552.5 – 3552.6 MeV.

3. Sensitivity of observing the $J_\tau(nS)$ and uncertainty of τ mass measurement

Next, we estimate the sensitivity of observing the $J_\tau(nS)$ at a future high luminosity facility such as the super tau-charm facility (STCF) in China [39] and the super charm-tau factory (SCTF) in Russia [40]. To determine which energy points are optimal for the study, we use the χ^2 values per integrated luminosity as

$$\frac{\chi_i^2}{\mathcal{L}_i} = \frac{(\sigma_i^{\text{total}}(m_\tau^{\text{PDG}}) - \sigma_i^{\text{con.}}(m_\tau))^2 \cdot \varepsilon_{X^+Y^-\cancel{E}}}{\sigma_i^{\text{total}}(m_\tau^{\text{PDG}})}, \quad (7)$$

where $\sigma_i^{\text{total}}(m_\tau^{\text{PDG}}) = \sigma(W, m_\tau, \Gamma_\tau, \delta_W)$ in Eq. (1) is the total cross section for energy point i assuming $m_\tau = m_\tau^{\text{PDG}}$, $\sigma_i^{\text{con.}}$ is the cross section when only the continuum is included in Eq. (2), $\varepsilon_{X^+Y^-\cancel{E}} = 8\%$ is the reconstruction efficiency of $e^+e^- \rightarrow X^+Y^-\cancel{E}$ events [25, 39], and \mathcal{L}_i is the integrated luminosity. The reconstruction efficiency is estimated based on Monte Carlo simulations, where KKMC [41, 42] is used to simulate the production of τ pairs, and TAUOLA [43, 44] is used to generate all the τ decay modes. Note that in the calculation of $\sigma_i^{\text{con.}}(m_\tau)$, m_τ is allowed to vary so that $\frac{\chi_i^2}{\mathcal{L}_i}$ has different values at each energy point. Here, we choose the best solution by minimizing the value of $\sum_i \frac{\chi_i^2}{\mathcal{L}_i}$ within the region of $3.54 < W < 3.56$ GeV. In the end, we find the values of $\frac{\chi_i^2}{\mathcal{L}_i}$ are relatively large at $W = 3552.56$ and 3555.83 MeV, and

that at 3552.56 MeV is about half of that at 3555.83 MeV. Besides the above two energy points, an additional energy point of 3549.00 MeV is needed to obtain the whole lineshape of the $e^+e^- \rightarrow X^+Y^-\cancel{E}$ cross section.

We determine how large data samples are required in order to observe the $J_\tau(nS)$ at $W = 3549.00$, 3552.56 , and 3555.83 MeV by performing 10^5 sets of simulated pseudoexperiments with the reconstruction efficiencies of $\varepsilon_{X^+Y^-\cancel{E}} = (8.0 \pm 0.2)\%$ [25, 39] and $\varepsilon_{\mu^+\mu^-} = (45.00 \pm 0.01)\%$ [39, 45], and other quantities used in Eq. (3). Since the energy difference between energy points two and three is very small, we expect the efficiencies at these two points are very similar and almost 100% correlated. The significance of the observation of the tauonium is independent of the uncertainty of the efficiency. The numbers of expected events for $e^+e^- \rightarrow X^+Y^-\cancel{E}$ and $e^+e^- \rightarrow \mu^+\mu^-$ in simulated data samples are determined by $N_{X^+Y^-\cancel{E}}^{\text{data}} = \sigma^{\text{total}}(m_\tau^{\text{PDG}}) \cdot \mathcal{L} \cdot \varepsilon_{X^+Y^-\cancel{E}}$ and $N_{\mu^+\mu^-}^{\text{data}} = \sigma^{\mu^+\mu^-} \cdot \mathcal{L} \cdot \varepsilon_{\mu^+\mu^-}$. The statistical uncertainties of $N_{X^+Y^-\cancel{E}}^{\text{data}}$ and $N_{\mu^+\mu^-}^{\text{data}}$ are the square roots of them. For $e^+e^- \rightarrow X^+Y^-\cancel{E}$ at $W = 3549.00$ MeV, since the signal yield (N) is small, the statistical uncertainty of N is estimated with the Bayesian approach implemented in the Bayesian Poisson Upper Limit Estimator at a 68.27% confidence level [46], where the number of expected background events is zero. The numbers of expected events and the statistical uncertainties for $e^+e^- \rightarrow X^+Y^-\cancel{E}$ and $e^+e^- \rightarrow \mu^+\mu^-$ in the simulated data samples are summarized in Table 2, where the integrated luminosities are optimized and determined based on the χ^2 value to estimate the $J_\tau(nS)$ signal significance reaching a 5σ level (discussed below). For each set of pseudoexperiment, we generate randomly the numbers of events ($N_{X^+Y^-\cancel{E},i}^{\text{data}}$ and $N_{\mu^+\mu^-,i}^{\text{data}}$, $i = 1, 2, \text{ and } 3$) according to Poisson distributions.

TABLE 2: Numbers of $e^+e^- \rightarrow X^+Y^-\cancel{E}$ and $\mu^+\mu^-$ events and their statistical uncertainties in the pseudoexperiments with $m_\tau = m_\tau^{\text{PDG}}$.

i	\mathcal{L}_i (fb $^{-1}$)	W_i (MeV)	$N_{X^+Y^-\cancel{E},i}^{\text{data}}$	$N_{\mu^+\mu^-,i}^{\text{data}}$
1	5	3549.00	$0.1^{+1.2}_{-0.1}$	$(1.1764 \pm 0.0003) \times 10^7$
2	500	3552.56	$(8.772 \pm 0.009) \times 10^5$	$(1.17394 \pm 0.00003) \times 10^9$
3	1000	3555.83	$(2.4052 \pm 0.0005) \times 10^7$	$(2.34331 \pm 0.00005) \times 10^9$

A least-square fit is applied to each set of the pseudoexperiments with

$$\chi^2 = \sum_{i=1}^3 \left(\frac{\mathcal{R}_i^{\text{data}} - \hat{\mathcal{R}}_i(m_\tau)}{\Delta \mathcal{R}_i^{\text{data}}} \right)^2, \quad (8)$$

where $\mathcal{R}_i^{\text{data}} = \frac{N_{X^+Y^-\cancel{E},i}^{\text{data}}}{N_{\mu^+\mu^-,i}^{\text{data}}}$ and $\Delta \mathcal{R}_i^{\text{data}}$ is its statistical uncertainty calculated from those of $N_{X^+Y^-\cancel{E},i}^{\text{data}}$ and $N_{\mu^+\mu^-,i}^{\text{data}}$; $\hat{\mathcal{R}}_i(m_\tau)$ is the expected ratio at the τ mass m_τ to be determined from the fit. The fit to one pseudoexperiment is shown in Fig. 2a, and the corresponding contribution from the $J_\tau(nS)$ atom cross section (σ^{atom}) is shown in Fig. 2b. For 10^5 sets of simulated pseudoexperiments, the average value of χ^2/ndf is 0.7/2, where ndf is the number of degrees of freedom. This indicates a very good fit to the simulated data samples.

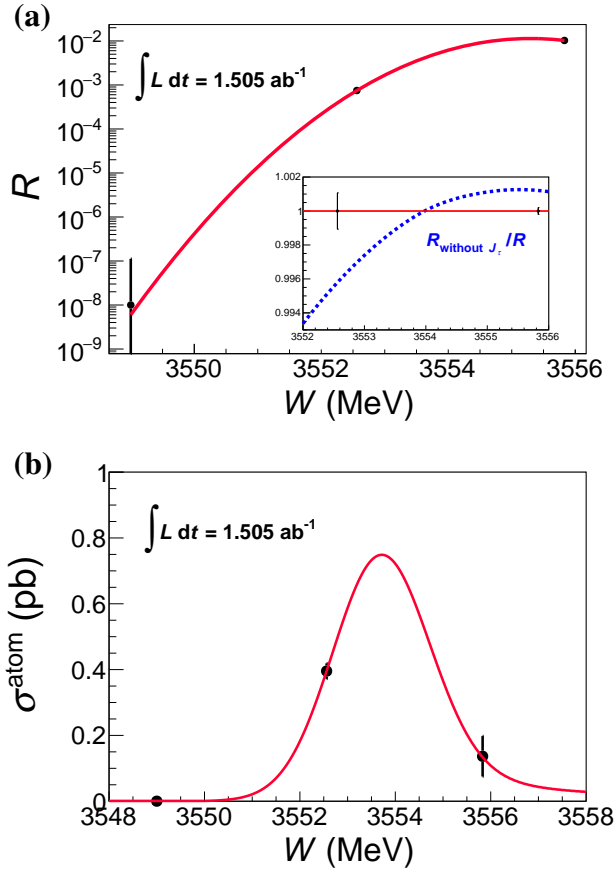


FIG. 2: (a) The fit to $\mathcal{R}^{\text{data}}$ from one set of pseudoexperiment data, and (b) the σ^{atom} contribution from the fit. The dots with error bars are the pseudoexperiment data, and the red curves display the best fit. The blue dashed line in the inset of (a) shows $\mathcal{R}_{\text{without } J_\tau}/\mathcal{R}$.

By removing the $J_\tau(nS)$ atom contribution in calculating $\hat{\mathcal{R}}_\tau(m_\tau)$ and refitting the data, we find a much poorer fit quality (the average value of χ^2/ndf is 51/2 for the 10^5 sets of simulated pseudoexperiments) and the difference in the χ^2 s measures the statistical significance of the $J_\tau(nS)$ signals. Figure 3 shows the normalized distribution of the statistical significances in all the pseudoexperiments. We conclude that in the scenario of taking 5 fb^{-1} data at 3549.00 MeV, 500 fb^{-1} at 3552.56 MeV, and 1000 fb^{-1} at 3555.83 MeV as indicated in Table 2, we have a 96% chance of discovering the $J_\tau(nS)$ with a statistical significance larger than 5σ and an almost 100% chance of observing it with a significance larger than 3σ . These data samples correspond to about 350 and 175 days' data taking time at the STCF [39] and SCTF [40], with designed instantaneous luminosities of 0.5×10^{35} and $1.0 \times 10^{35} \text{ cm}^{-2}\text{s}^{-1}$, respectively. Here, we assume the efficiency and δ_W at the SCTF are the same as those at the STCF. If the δ_W is reduced to 0.1 MeV, the required integrated luminosity of the data is only 66 fb^{-1} . In order to minimize the impact of beam energy instability and detector performance, it is advisable to frequently measure the beam energy and collect data at two high energy points in multiple rounds, with

the integrated luminosity ratio of 1:2, rather than completing data collection at one energy before moving to the other.

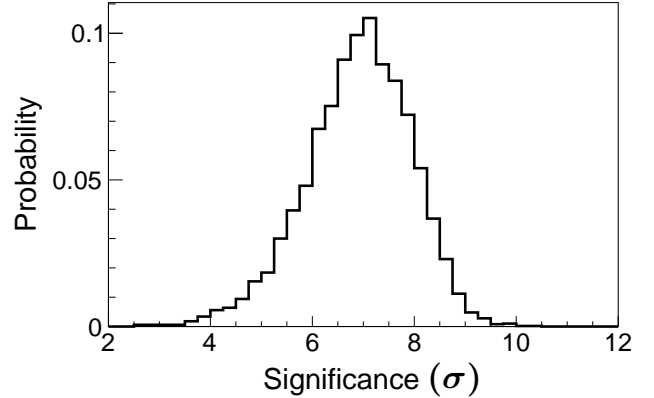


FIG. 3: Normalized distribution of the statistical significance of the $J_\tau(nS)$ signals in all the pseudoexperiments.

The background cross section can be measured at W_1 . The background cross section $\sigma_B = 0^{+0.12} \text{ pb}$ is obtained at BESIII [25]. If we set $\sigma_B = 0.12/2 \text{ pb}$ in data, and σ_B and m_τ float in the fit, $\Delta\chi_{J_\tau}^2/\text{ndf} = 45.4/1$ with the significance of 6.7σ is obtained, where $\Delta\chi_{J_\tau}^2 = \chi_{\text{without } J_\tau}^2 - \chi_{J_\tau}^2$. Taking into account the non- τ background, i.e. changing the number of background events to be 10_{-10}^{+120} (corresponding to an integrated luminosity of 500 fb^{-1}) for the second point and 20_{-20}^{+240} (corresponding to an integrated luminosity of 1000 fb^{-1}) for third energy point, an average signal significance of the J_τ is reduced by 0.02σ from 6.8σ . The ratios of the numbers of non- τ backgrounds including the uncertainty based on the BESIII cross section determination [25] relative to the numbers of $e^+e^- \rightarrow X^+Y^-\cancel{E}$ are 1.5×10^{-4} and 1.1×10^{-5} at $W = 3552.56$ and 3555.83 MeV , respectively. Therefore, the non- τ backgrounds are negligible.

With these data samples, we obtain a high precision τ mass measurement. The above fit yields

$$m_\tau = (1\,776\,860.00 \pm 0.25 \text{ (stat.)} \pm 0.99 \text{ (syst.)}) \text{ keV},$$

where the first and second uncertainties are statistical and systematic, respectively. The fit with the $J_\tau(nS)$ contribution removed gives a shift of -4 keV relative to the nominal fit with both the bound state and continuum contributions. This shift is about a factor of 4 larger than the total uncertainty and should not be ignored in the future high precision measurements.

4. Systematic uncertainties

The systematic uncertainties in the τ mass measurement are listed in Table 3. The uncertainty of the center-of-mass energy scale W is estimated according to that achieved twenty years ago at the VEPP-4M, which had a characteristic uncertainty of 1.5 keV in the beam energy in the $\psi(2S)$ and

J/ψ mass scan experiments using the resonant depolarization method [47, 48]. The uncertainty of W_2 (W_3) is estimated to be $1.5\sqrt{2} = 2.12$ keV, leading to an uncertainty of 0.72 (0.35) keV in m_τ .

The energy spread can be measured from experimental data directly. In the previous measurements, the m_τ uncertainties from energy spread and energy scale are 16 keV and $^{+22}_{-86}$ keV from BESIII [25], and 25 keV and 40 keV from KEDR [28]. Therefore, we conservatively take the maximum ratio of $16/22 \sim 0.73$, and find the uncertainty in the m_τ measurement from energy spread is $0.73 \times \sqrt{0.72^2 + 0.35^2} = 0.59$ keV, where the 0.72 and 0.35 keV are the m_τ uncertainties from energy scales at W_2 and W_3 , respectively. In the m_τ measurements at the BESIII [25] and the KEDR [28] experiments, δ_W is fit from $\delta_{m_{\psi(2S)}}$ and $\delta_{m_{J/\psi}}$, where $\delta_{m_{\psi(2S)}}$ and $\delta_{m_{J/\psi}}$ are free parameters and are obtained from fits to the measured $\psi(2S)$ and J/ψ excitation curves [48]. If we consider δ_W as a free parameter in the m_τ fit function in Eq. (8), the 0.27 keV uncertainty of m_τ is given through $\Delta m_\tau^2|_{\chi^2=2} - \Delta m_\tau^2|_{\chi^2=1}$.

Considering the improvement of the particle identifications for e , μ , π , K , and ρ candidates at the future experiments, we expect the efficiency and its uncertainty of $\varepsilon_{X^+Y^-\mathbb{E}} = (8.0 \pm 0.2)\%$. We change the efficiency by $\pm 1\sigma$, and find a change of 0.04 keV on the τ mass compared with the nominal result.

By replacing the NLO correction with the NNLO correction in the calculation of the $e^+e^- \rightarrow X^+Y^-\mathbb{E}$ cross sections, we find the τ mass changes by 0.07 keV which is included as the uncertainty due to the theoretical accuracy. Since we perform the fit to the ratio of observed $e^+e^- \rightarrow X^+Y^-\mathbb{E}$ and $\mu^+\mu^-$ events, the uncertainty from the integrated luminosity is cancelled. For the first energy point with a small expected number of events and large statistical uncertainty, we enlarge the uncertainty on the $N_{X^+Y^-\mathbb{E}}^{\text{data}}$ by a factor of three, and the resulting τ mass does not change.

Assuming all these sources are independent, we add them in quadrature to obtain the total systematic uncertainty, which is listed in Table 3. Taking into account the systematic uncertainties mentioned above, we obtain an average signal significance of the J_τ of 6.7σ , which will be 6.8σ if the systematic uncertainties are not taken into account.

TABLE 3: The systematic uncertainties of the m_τ (σ_{m_τ}) in keV.

Sources	σ_{m_τ} (keV)
Energy scale of W_2	0.72
Energy scale of W_3	0.35
Energy spread δ_W	0.59
Efficiency	0.04
Theory	0.07
Systematic uncertainties	0.99

The value of m_τ^{Natural} may be different from the central value of $m_\tau^{\text{PDG}} = 1776.86$ MeV [22]. We examine the statistical significance of the $J_\tau(nS)$ signals as a function of the difference

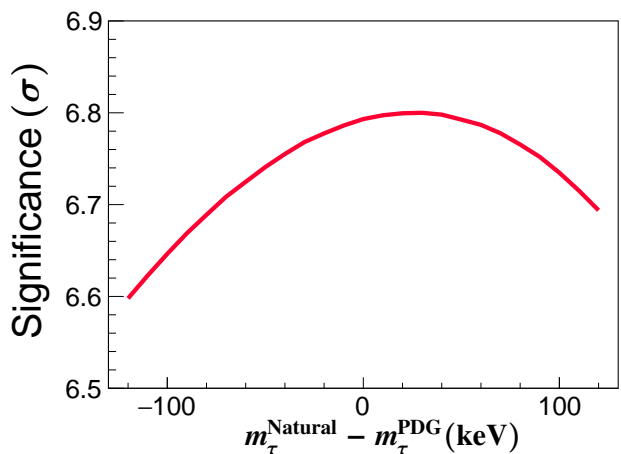


FIG. 4: The significance of $J_\tau(nS)$ as a function of $m_\tau^{\text{Natural}} - m_\tau^{\text{PDG}}$.

$m_\tau^{\text{Natural}} - m_\tau^{\text{PDG}}$ as shown in Fig. 4, and find that the uncertainty in m_τ remains unchanged, since it is mainly determined by the beam properties.

5. Conclusion

To conclude, the novel method proposed in this Letter is summarized as follows: (1) In contrast to the process $e^+e^- \rightarrow J_\tau \rightarrow \mu^+\mu^-$ proposed in Ref. [24], the continuum contributions are much smaller and the selected τ pair candidate sample is very pure in the process $e^+e^- \rightarrow J_\tau \rightarrow \tau^+\tau^-$. The signal to background ratio in $e^+e^- \rightarrow J_\tau \rightarrow \tau^+\tau^-$ is improved drastically. (2) We propose to measure the relative rate $\mathcal{R} = \frac{N_{X^+Y^-\mathbb{E}}}{N_{\mu^+\mu^-}}$ rather than the absolute cross section so that the uncertainties are controlled at a low level since those in VP, ISR, and luminosity determinations are canceled. (3) m_τ is taken as a free parameter to be extracted from the experimental data. A high precision m_τ measurement can be achieved at the same time.

In summary, we show that the $\tau^+\tau^-$ atom with $J^{PC} = 1^{--}$, J_τ , can be observed with a significance larger than 5σ with a 1.5 ab^{-1} data sample at the proposed high luminosity experiments STCF and SCTF, by measuring the cross section ratio of the processes $e^+e^- \rightarrow X^+Y^-\mathbb{E}$ and $e^+e^- \rightarrow \mu^+\mu^-$. With the same data sample, the τ lepton mass can be measured with a precision of 1 keV, a factor of about 100 improvement over the existing world best measurements.

Acknowledgments

We thank Profs. Kuang-Ta Chao and Hua-Sheng Shao for valuable and helpful discussions. This work is supported in part by National Key Research and Development Program of China under Contract No. 2020YFA0406300, National Natural Science Foundation of China (NSFC) under contract No. 11975076, No. 12161141008, No. 12135005, No. 12075018, No. 12005040, and No. 12335004; and the Fundamental Research Funds for the Central Universities

Grant No. RF1028623046.

Author contributions

Yu-Jie Zhang proposed this project. Jing-Hang Fu and Yu-Jie Zhang did the calculations. Sen Jia, Xing-Yu Zhou,

Cheng-Ping Shen, and Chang-Zheng Yuan carried out the experiments. Cheng-Ping Shen and Chang-Zheng Yuan checked the results and resolved physical and technical issues. Yu-Jie Zhang, Cheng-Ping Shen and Chang-Zheng Yuan supervised throughout this work. All authors contributed to the writing of the manuscript.

-
- [1] S. G. Karshenboim. Precision physics of simple atoms: QED tests, nuclear structure and fundamental constant. *Phys Rept* 2005;422:1-63.
- [2] M. S. Safronova, D. Budker, D. DeMille, et al. Search for new physics with atoms and molecules. *Rev Mod Phys* 2018;90:025008.
- [3] V. W. Hughes, M. Grosse Perdekamp, D. Kawall, et al. Test of CPT and Lorentz invariance from muonium spectroscopy. *Phys Rev Lett* 2001;87:111804.
- [4] T. Yamazaki, T. Namba, S. Asai, et al. Search for CP violation in positronium decay. *Phys Rev Lett* 2010;104:083401 [Erratum: *Phys Rev Lett* 2018;120:239902].
- [5] MAGE Collaboration, A. Antognini, et al. Studying Antimatter Gravity with Muonium. *Atoms* 2018;6:17.
- [6] A. Soter, A. Knecht. Development of a cold atomic muonium beam for next generation atomic physics and gravity experiments. *SciPost Phys Proc* 2021;4:031.
- [7] W. Bernreuther, U. Löw, J. P. Ma, et al. How to test CP, T, and CPT invariance in the three photon decay of polarized 3S_1 wave triplet positronium. *Z Phys C* 1988;41:143-158.
- [8] G. S. Adkins, D. B. Cassidy, J. Pérez-Ríos. Precision spectroscopy of positronium: Testing bound-state QED theory and the search for physics beyond the Standard Model. *Phys Rept* 2022;975:1-61.
- [9] S. C. Ellis, J. Bland-Hawthorn. Astrophysical signatures of leptonium. *Eur Phys J D* 2018;72:18.
- [10] M. Deutsch. Evidence for the formation of positronium in gases. *Phys Rev* 1951;82:455-456.
- [11] V. W. Hughes, D. W. McColm, K. Ziock, et al. Formation of muonium and observation of its Larmor precession. *Phys Rev Lett* 1960;5:63-65.
- [12] P. J. Fox, S. R. Jindariani, V. D. Shiltsev. DIMUS: supercompact Dimuonium Spectroscopy collider at Fermilab. *J Instrum* 2023;18:T08007.
- [13] R. Gargiulo, E. Di Meo, D. Paesani, et al. True muonium resonant production at e^+e^- colliders with standard crossing angle. *J Phys G* 2024;51:045004.
- [14] S. J. Brodsky, R. F. Lebed. Production of the smallest QED atom: True muonium $\mu^+\mu^-$. *Phys Rev Lett* 2009;102:213401.
- [15] U. D. Jentschura, G. Soff, V. G. Ivanov, et al. Bound $\mu^+\mu^-$ system. *Phys Rev A* 1997;56:4483-4495.
- [16] J. W. Moffat. Does a Heavy Positronium Atom Exist?. *Phys Rev Lett* 1975;35:1605-1606.
- [17] C. Avilez, R. Montemayor, M. Moreno. Tauonium: $\tau^+\tau^-$, a bound state of heavy leptons. *Lett Nuovo Cim* 1978;21:301-304.
- [18] C. Avilez, E. Ley Koo, M. Moreno. Comments on the observability of tauonium. *Phys Rev D* 1979;19:2214.
- [19] D. d'Enterria, R. Perez-Ramos, H.-S. Shao. Ditaonium spectroscopy. *Eur Phys J C* 2022;82:923.
- [20] G. Yu, Y. Cai, Q. Gao, et al. Production of positronium, dimuonium, and ditaonium in ultra-peripheral heavy ion collisions with two-photon processes. [arXiv:2209.11439 \[hep-ph\]](https://arxiv.org/abs/2209.11439).
- [21] D. d'Enterria, H.-S. Shao. Observing true tauonium via two-photon fusion at e^+e^- and hadron colliders. *Phys Rev D* 2022;105:093008.
- [22] Particle Data Group Collaboration, R. L. Workman, et al. Review of Particle Physics. *Prog Theor Exp Phys* 2022;2022:083C01.
- [23] A. A. Malik, I. S. Satsunkevich. Production of $(\tau^+\tau^-)$ in electron positron collisions. *Int J Mod Phys A* 2009;24:4039-4044.
- [24] D. d'Enterria, H.-S. Shao. Prospects for ditaonium discovery at colliders. *Phys Lett B* 2023;842:137960.
- [25] BESIII Collaboration, M. Ablikim, et al. Precision measurement of the mass of the τ lepton. *Phys Rev D* 2014;90:012001.
- [26] BESIII Collaboration, J. Y. Zhang, et al. τ lepton mass measurement at BESIII. *SciPost Phys Proc* 2019;1:004.
- [27] M. N. Achasov, X. H. Mo, N. Y. Muchnoi, et al. Tau mass measurement at BESIII. *EPJ Web Conf* 2019;212:08005.
- [28] V. V. Anashin, et al. Measurement of the τ lepton mass at the KEDR detector. *JETP Lett* 2007;85:347-352.
- [29] E. Oset, L. R. Dai, L. S. Geng. Repercussion of the $a_0(1710)$ [$a_0(1817)$] resonance and future developments. *Sci Bull* 2023;243-246.
- [30] X. G. He, J. Tandean, G. Valencia. Pursuit of CP violation in hyperon decays at e^+e^- colliders. *Sci Bull* 2022;67:1840-1843.
- [31] Z. Q. Liu and R. E. Mitchell. New hadrons discovered at BESIII. *Sci Bull* 2023;68:2148-2150.
- [32] W. J. Marciano, A. Sirlin. Electroweak radiative corrections to τ decay. *Phys Rev Lett* 1988;61:1815-1818.
- [33] Belle II Collaboration, I. Adachi, et al. Measurement of the τ -lepton mass with the Belle II experiment. *Phys Rev D* 2023;108:032006.
- [34] E. A. Kuraev, V. S. Fadin. On radiative corrections to e^+e^- single photon annihilation at high-energy. *Sov J Nucl Phys* 1985;41:466-472.
- [35] S. Actis, et al. (Working Group on Radiative Corrections and Monte Carlo Generators for Low Energies). Quest for precision in hadronic cross sections at low energy: Monte Carlo tools vs. experimental data. *Eur Phys J C* 2010;66:585-686.
- [36] K. Dzikowski, O. D. Skoromnik. A generating integral for the matrix elements of the coulomb green's function with the coulomb wave functions. *J Math Phys* 2022;61:032103.
- [37] BESIII Collaboration, M. Ablikim, et al. Measurement of the Cross Section for $e^+e^- \rightarrow$ Hadrons at Energies from 2.2324 to 3.6710 GeV. *Phys Rev Lett* 2022;128:062004.
- [38] M. B. Voloshin. The Onset of $e^+e^- \rightarrow \tau^+\tau^-$ at threshold revisited. *Phys Lett B* 2003;556:153-162.
- [39] M. Achasov, X. C. Ai, L. P. An, et al. STCF conceptual design report (Volume 1): Physics & detector. *Front Phys* 2024;19:14701.
- [40] M. N. Achasov, V. E. Blinov, A. V. Bobrov, et al. Experiments at the Super Charm-Tau factory. *Phys Usp* 2024;67:55-70.
- [41] S. Jadach, B. F. L. Ward, Z. Wąs. The precision Monte Carlo

- event generator \mathcal{KK} for two fermion final states in e^+e^- collisions. [Comput Phys Commun 2000;130:260-325](#).
- [42] S. Jadach, B. F. L. Ward, Z. Wąs. Coherent exclusive exponentiation for precision Monte Carlo calculations. [Phys Rev D 2001;63:113009](#).
- [43] S. Jadach, J. H. Kühn, Z. Wąs. TAUOLA - a library of Monte Carlo programs to simulate decays of polarized τ leptons. [Comput Phys Commun 1990;64:275-299](#).
- [44] S. Jadach, Z. Wąs, R. Decker, et al. The τ decay library TAUOLA, version 2.4. [Comput Phys Commun 1993;76:361-380](#).
- [45] BESIII Collaboration, M. Ablikim, et al. Measurement of cross sections for $e^+e^- \rightarrow \mu^+\mu^-$ at center-of-mass energies from 3.80 to 4.60 GeV. [Phys Rev D 2020;102:112009](#).
- [46] Y. S. Zhu. Upper limit for Poisson variable incorporating systematic uncertainties by Bayesian approach. [Nucl Instrum Meth A 2007;578:322-328](#).
- [47] KEDR Collaboration, V. M. Aulchenko, et al. New precision measurement of the J/ψ and ψ' meson masses. [Phys Lett B 2003;573:63-79](#).
- [48] KEDR Collaboration, V. V. Anashin, et al. Final analysis of KEDR data on J/ψ and $\psi(2S)$ masses. [Phys Lett B 2015;749:50-56](#).